

# Synthesis And Characterization Of A Ni(II) Complex Derived From The Schiff Base (*E*)-2-((1*H*-Imidazol-4-*Yl*)Methylene)Hydrazine-1-Carbothioamide

Seydou Sané<sup>a</sup>, Mbossé Ndiaye Gueye<sup>a</sup>, Gorgui Awa Seck<sup>a</sup>,  
Ibrahima Elhadji Thiam<sup>a</sup>, Ousmane Diouf<sup>a</sup>, Mohamed Gaye<sup>a\*</sup> Pascal Retailleau<sup>b</sup>

<sup>a</sup>Department of Chemistry, University Cheikh Anta Diop, Dakar, Sénégal

<sup>b</sup>Centre de Recherche de Gif, Institut de Chimie des Substances Naturelles, CNRS-UPR2301, 1 Avenue la Terrasse, 91198 Gif sur Yvette, France

## Abstract:

The reaction of 1-((1*H*-imidazol-4-*yl*)methylene)thiosemicarbazide (*HL*) with NiCl<sub>2</sub>·6H<sub>2</sub>O in 2:1 ratio has yielded a mononuclear formulated as [Ni(*HL*)<sub>2</sub>].2Cl. The structure of the complex was solved by single crystal X-ray crystallography. The asymmetric unit of the mononuclear complex is composed by one Ni<sup>2+</sup> ion, two neutral molecules of ligand and two chloride anions. Each ligand molecule acts in tridentate fashion yielding a hexacoordinated Ni(II) ion with an environment best described as a octahedral geometry. Complex 1 crystallizes in the monoclinic space group *P* $\bar{1}$  with the following parameters: *a* = 8.17376(16) Å, *b* = 9.17460(15) Å, *c* = 13.2716(2) Å,  $\alpha$  = 95.1157(14)°,  $\beta$  = 107.0840(16)°,  $\gamma$  = 101.2883(15), *V* = 921.44(3) Å<sup>3</sup>, *Z* = 2, *R*<sub>1</sub> = 0.0208, *wR*<sub>2</sub> = 0.054. The supramolecular structure is consolidated by multiple hydrogen bonds.

**Keywords:** Schiff base, crystal, complex, copper, octahedral, mononuclear

Date of Submission: 01-10-2023

Date of Acceptance: 10-10-2023

## I. Introduction

Due to their varied biological properties, thiosemicarbazones are widely studied. Some of these compounds exhibit antitumor [1–3], antiviral [4, 5], antimicrobial [6, 7], and antimalarial [8, 9] properties. Some of these properties can be enhanced by the coordination of these molecules to transition metals. Schiff bases derived from thiosemicarbazide were used for preparing a wide range of coordination complexes with interesting physical properties [10–12]. In addition to the physical properties, the coordination complexes present more important biological properties [13–16] on comparison to the biological properties of organic ligands which generate these compounds. These complexes often present original molecular structures owing to the different coordination modes depending on the topology of these Schiff bases [17–20]. Indeed, the thiosemicarbazide fragment can be complexed in various ways owing to the possibility of a thione/thiol equilibrium which can be established. Thus, the sulfur atom can bind to the metal in its thione form or in its thiolate form or remains free [21–24]. Consequently, the complexes prepared can present several types of physical properties such as magnetism [25, 26], fluorescence [27, 28] or catalytic [29, 30] as reported. The aim of this study is to synthesize a new ligand 1-((1*H*-imidazol-4-*yl*)methylene)thiosemicarbazide (*HL*) and its nickel (II) complex and to present a structural analysis of the synthesized compounds (Fig. 1). Infrared, <sup>1</sup>H and <sup>13</sup>C NMR spectroscopies and X-ray diffraction were used in the experimental determination of the structures of the ligand and the complex (Scheme 1).

## II. Material And Methods

### Materials and Procedures

4*H*-imidazole-2-carbaldehyde, thiosemicarbohydrazide, as well as NiCl<sub>2</sub>·6H<sub>2</sub>O were commercial products from Aldrich and were used without further purification. Solvents were of reagent grade and were purified by the usual methods. Elemental analyzes were performed in a Carlo-Erba EA microanalyzer. Infrared spectra were recorded on a Perkin Elmer Spectrum Two spectrophotometer (4000–400 cm<sup>-1</sup>). The <sup>1</sup>H and <sup>13</sup>C NMR spectra of the Schiff base were recorded in MeOD-*d*<sub>4</sub> on a Bruker 250 MHz spectrometer at room temperature using TMS as internal reference. The UV–Vis spectra were recorded in acetonitrile solution concentration of 10<sup>-3</sup> M at 25 °C on a Perkin Elmer Lambda 365 UV–Vis spectrophotometer. The molar

\* Corresponding author: mohamedl.gaye@ucad.edu.sn

conductance of  $10^{-3}$  M solution of the metal complex in acetonitrile was measured at 25° C using a WTW LF-330 conductivity meter with a WTW conductivity cell. Room-temperature magnetic susceptibility of the powdered sample was measured using a Johnson Matthey scientific magnetic susceptibility balance (calibrant  $\text{Hg}[\text{Co}(\text{SCN})_4]$ ).

**Synthesis of the Schiff base ligand 1-((1*H*-imidazol-4-yl)methylene)thiosemicarbazide (HL)**

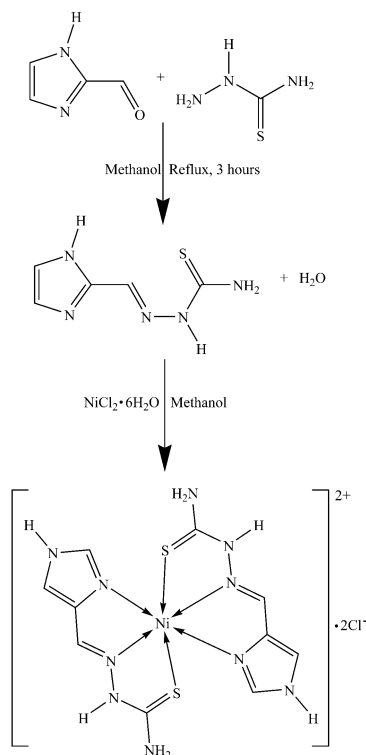
To a round bottomed flask, 20 mL of methanol and thiosemicarbazide (0.9114 g, 10 mmol) were added successively and stirred. After the dissolution of the compound, 4*H*-imidazole-2-carbaldehyde (0.9609 g, 10 mmol) and two drops of glacial acetic acid were added. The resulting mixture was refluxed for three hours. On cooling, the white precipitate, which appears, was recovered by filtration, and successively washed with cold methanol (2 x 10 mL) and diethyl ether (2 x 10 mL), before being dried in open air. Yield: 92%. M.P : 170° C. Anal. calcd. for  $\text{C}_5\text{H}_7\text{N}_3\text{S}$ : % C, 35.49; % H, 4.17; % N, 41.39; S, 18.95. Found % C, 35.47; % H, 4.19; % N, 41.36; S, 18.91. FTIR: ( $\nu$ ,  $\text{cm}^{-1}$ ) : 3385, 3200, 1692, 1615, 1516, 1259, 795.  $^1\text{H}$  NMR (MeOD- $d_4$ ,  $\delta$ (ppm)): 7.94 (S, 1H, **H**— $\text{N}_{\text{hydrazino}}$ ), 7.84 (S, 1H, **CH=N**), 7.56 (S, 1H, **H**— $\text{N}_{\text{imidazol}}$ ), 7.45 (S, 1H, **H**— $\text{C}_{\text{imidazol}}$ ), 7.23 (S, 1H, **H**— $\text{C}_{\text{imidazol}}$ ), 4.95 (S, 2H, **H**<sub>2</sub>N—).  $^{13}\text{C}$  NMR (MeOD- $d_4$ ,  $\delta$ (ppm)) : 178.48, 137.12, 134.95, 122.70, 120.66.

**Synthesis of the complex**

A methanolic (10 mL) solution of  $\text{NiCl}_2 \cdot 6\text{H}_2\text{O}$  (0.1189 g, 0.5 mmol) was added to a flask containing a solution of HL (0.0846 g, 0.5 mmol) dissolved in 10 mL of methanol. The mixture was refluxed for one hour. Upon cooling, the solution was filtered and left to slow evaporation. Blue crystals suitable for X-ray analyzes were recovered after a week. Yield : 68.8 % . Anal. calcd. for  $\text{NiC}_{10}\text{H}_{14}\text{N}_{10}\text{Cl}_2\text{S}_2$ : . Found % C 25.66; % H 3.02; % N 29.93; % Cl 15.15; S 13.70. Found % C 25.64; % H 3.00; % N 29.90; % Cl 15.13; S 13.72. FTIR: ( $\nu$ ,  $\text{cm}^{-1}$ ) : 3380, 3203, 1605, 1240, 759. MP > 260.

**X-ray data collection structure determination and refinement**

Single crystals of  $\text{C}_{10}\text{H}_{14}\text{NiN}_{10}\text{Cl}_2\text{S}_2$  were grown by slow evaporation of MeOH solution of the complex. A suitable crystal was selected and mounted on a XtaLAB Synergy, Dualflex, Hypix diffractometer Radiation with graphite monochromatized  $\text{MoK}\alpha$  radiation ( $\lambda = 0.710173$ ). Data were collected at the temperature of 100 K. Details of the X-ray crystal structure solution and refinement are given in Table 1. The structure was solved with the SHELXT [31] structure solution program using direct methods and refined with the SHELXTL [32] software package. The hydrogen atoms of NH groups were located in the Fourier difference maps and refined. Molecular graphics were generated using ORTEP [33].



**Scheme 1.** Synthesis procedure of the ligand and the complex  $[\text{Ni}(\text{HL})_2] \cdot 2\text{Cl}$ .

**Table-1.** Crystal data and details of the structure determination of the complex.

Empirical formula	C <sub>10</sub> H <sub>14</sub> N <sub>10</sub> Cl <sub>2</sub> NiS <sub>2</sub>
Formula weight (g/mol)	468.04
Crystal system	Triclinic
Space group	<i>P</i> $\bar{1}$
Crystal size (mm)	0.20 × 0.13 × 0.07
Mo K $\alpha$ (Å)	0.71073
Temperature (K)	100
<i>a</i> (Å)	8.17376(16)
<i>b</i> (Å)	9.17460(15)
<i>c</i> (Å)	13.2716(2)
$\alpha$ (°)	95.1157(14)
$\beta$ (°)	107.0840(16)
$\gamma$ (°)	101.2883(15)
<i>V</i> (Å <sup>3</sup> )	921.44(3)
<i>Z</i>	2
<i>D</i> <sub>cal</sub> (g cm <sup>-3</sup> )	1.687
F(000)	476
$\mu$ (mm <sup>-1</sup> )	1.59
$\omega$ <sub>max</sub> (°)	34.1880
<i>h, k, l</i> ranges	-10 ≤ <i>h</i> ≤ 10, -11 ≤ <i>k</i> ≤ 10, -16 ≤ <i>l</i> ≤ 16
Measured reflections	22511
Independent reflections	3768
Reflections [ <i>I</i> > 2 $\sigma$ ( <i>I</i> )]	3604
<i>R</i> <sub>int</sub>	0.036
<i>R</i> [ <i>I</i> > 2 $\sigma$ ( <i>I</i> )]	0.020
<i>wR</i> <sub>2</sub>	0.054
Data/parameters/restraints	3604/226/0
Goodness-of-Fit	1.05
$\Delta\rho$ <sub>max</sub> , $\Delta\rho$ <sub>min</sub> (e Å <sup>-3</sup> )	0.69, -0.26

### III. Results and discussions

#### General studies

Reaction of nickel(II) chloride and HL in 1:2 ratio in methanol produces the mononuclear nickel(II) complex [Ni(HL)<sub>2</sub>].2Cl (Figure 1). The infrared spectrum of the ligand 1-((1*H*-imidazol-4-yl)methylene)thiosemicarbazide (HL) shows the presence of two bands pointed at 3385 cm<sup>-1</sup> and 3200 cm<sup>-1</sup> which are, respectively, assigned to  $\nu$ (NH<sub>2</sub>) and  $\nu$ (NH) vibrations of the ligand [34–36]. The bands due to the imidazole ring are pointed at 1615 cm<sup>-1</sup> and 1516 cm<sup>-1</sup> [37]. The  $\nu$ <sub>C=N</sub> appears at 1692 cm<sup>-1</sup>, while the characteristic bands due to the thioamide NH–C=S moiety are pointed at 1259 cm<sup>-1</sup> and 795 cm<sup>-1</sup>. The absence of the band characteristic of the S–H, expected at *ca.* 2600 cm<sup>-1</sup>, indicates that the compound is only in its thione form [38]. The <sup>1</sup>H NMR spectrum of the ligand recorded in CD<sub>3</sub>OD-*d*<sub>4</sub> shows a signal pointed at 7.94 ppm which is assigned to the proton of the hydrazinyl proton C=N–NH–. The proton of the azomethine group is pointed at 7.84 ppm. The protons –NH<sub>2</sub> gives signal at and 4.95 ppm. The signals due to the three protons of the imidazole ring appear

in the range 7.56–7.23 ppm. The  $^{13}\text{C}$  NMR spectrum of HL recorded in  $\text{CD}_3\text{OD}$  displays signal at 178.48 ppm which is characteristic of the carbon atom of the thiocarbonyl moiety. Signal due to the azomethine carbon atom is pointed at 173.89 ppm. The signals due to the carbon atoms of the imidazole ring are pointed at 134.95 ppm, 122.70 ppm and 120.66 ppm, respectively. The comparative study carried out between the infrared spectrum of the ligand and those of the complex reveals differences due to the coordination to the metal ion. The infrared spectrum of the resulting complex still shows bands attributed due to the  $-\text{NH}_2$  and  $-\text{NH}$ - groups with small shifts. This observation shows that the ligand acts in its neutral form in the complex. The  $\nu_{\text{C}=\text{N}}$  imine band appears on the nickel complex spectrum at  $1605\text{ cm}^{-1}$ , while the band of the  $\nu_{\text{C}=\text{N}}$  vibration of imidazole ring is pointed at  $1580\text{ cm}^{-1}$ . These strong shifts are due to the participation of the nitrogen atoms of the azomethine moiety and the imidazole ring of the ligand in the coordination to the metal ion [8, 9]. Additionally, the  $\text{C}=\text{S}$  bands undergo shift effect and appears at  $1240\text{ cm}^{-1}$  and  $759\text{ cm}^{-1}$ , indicating the involvement of the sulfur atom in the coordination to the nickel (II) cation [38]. In the electronic spectrum of the ligand, an intense band at 277 nm is attributed to the intraligand  $n \rightarrow \pi^*$  transition associated with the  $\text{C}=\text{N}$  and  $\text{C}=\text{S}$  groups. This band is present in the spectrum of the complex with a slight shift of the  $\lambda_{\text{max}}$ . The electronic spectrum of the Ni(II) complex displays additional bands at 239 nm due to  $\pi \rightarrow \pi^*$  transitions in the aromatic rings. The band at 284 nm is due to  $n \rightarrow \pi^*$  transition in  $\text{C}=\text{N}$  and  $\text{C}=\text{S}$  moieties. The band at 441 nm is attributed to the LMCT. The conductimetric measurement of the complex was carried out in a millimolar solution ( $10^{-3}\text{ M}$ ) of dimethylformamide. The value of the molar conductivity of the fresh solution ( $109\text{ S}\cdot\text{cm}^2\cdot\text{mol}^{-1}$ ) and of the solution after two weeks ( $115\text{ S}\cdot\text{cm}^2\cdot\text{mol}^{-1}$ ) shows a slight variation in conductivity which corresponds to a 2:1 electrolyte stable in DMF solution [39]. The  $\mu_{\text{eff}}$  value of the magnetic moment of  $2.87\ \mu_{\text{B}}$  at room temperature for the diamagnetic Ni(II) complex is indicative of the presence of one metal atom per molecule. The magnitude of  $\mu_{\text{eff}}$  is consistent with the expected magnetic moment for octahedral Ni(II) complexes of 2.8–3.3 BM for a  $d^8$  system with  $S = 1$  [40].

### Molecular Structure of Complex (1)

The complex crystallizes in the monoclinic system with the space group  $\text{P}2_1/\text{c}$ . Partially labelled plot of the mononuclear structure of Ni(II) complex is shown in Fig. 1. Selected interatomic distances are listed in Table 2. The structure of the complex is consistent with the  $[\text{Ni}(\text{HL})_2]\cdot 2\text{Cl}$  formulation. The asymmetric unit contains one  $\text{Ni}^{2+}$ , two neutral organic ligand, and two free chloride anions. The crystallographic study shows that the cation is formed with 1:2 [Ni:HL]. In the complex each Schiff base molecules acts in tridentate fashion through one azomethine nitrogen atom, one imidazole nitrogen atom and one thione sulfur atom resulting in two membered chelating rings NiNCCN and NiNNCS with bite angles of  $\text{N}6-\text{Ni}1-\text{N}8 = 78.30(5)^\circ$ ,  $\text{N}1-\text{Ni}1-\text{N}3 = 78.37(5)^\circ$ ,  $\text{S}1-\text{Ni}1-\text{N}3 = 80.80(4)^\circ$ ,  $\text{S}2-\text{Ni}1-\text{N}8 = 80.44(4)^\circ$ . The metal center is hexacoordinated, and the nickel (II) atom is in a severely distorted octahedral environment. The basal plane is occupied by N1, N6, S1 and S2 atoms, the apical positions being occupied by N3 and N8 atoms. The angles in the basal plane  $\text{N}1-\text{Ni}1-\text{N}6 = 88.41(5)^\circ$ ,  $\text{N}6-\text{Ni}1-\text{S}1 = 95.49(4)^\circ$ ,  $\text{S}1-\text{Ni}1-\text{S}2 = 92.75(1)^\circ$ ,  $\text{N}1-\text{Ni}1-\text{S}2 = 90.95(4)^\circ$ ,  $\text{N}1-\text{Ni}1-\text{S}1 = 159.14(4)^\circ$ ,  $\text{N}6-\text{Ni}1-\text{S}2 = 159.43(4)^\circ$  and the angles between the apical atoms  $\text{N}3-\text{Ni}1-\text{N}8 = 174.64(5)^\circ$  deviate severely from the ideal angles values of  $90^\circ$  and  $180^\circ$  for octahedral geometry. These facts are indicative of a severely distorted octahedral polyhedron around the Cu atom center. Each ligand form two five membered rings which are almost planar [NiSCNN (rms:  $0.0673\ \text{\AA}$  and  $0.0275\ \text{\AA}$ ) and NiNCCN (rms:  $0.0372\ \text{\AA}$  and  $0.0370\ \text{\AA}$ )]. In each ligand molecule, the two five membered rings issued from the coordination form dihedral angles of  $6.600(1)^\circ$  and  $3.533(1)^\circ$ , respectively. The Ni–S distances are respectively  $2.4662(5)\ \text{\AA}$  and  $2.4456(5)\ \text{\AA}$  and are consistent with those reported in the literature [38, 41]. The Ni–N(imidazole) bond lengths [ $2.082(1)\ \text{\AA}$  and  $2.094(1)\ \text{\AA}$ ] are slightly longer than the Ni–N(imine) distances [ $2.042(1)\ \text{\AA}$  and  $2.046(1)\ \text{\AA}$ ]. In the chain  $-\text{C}4-\text{N}3-\text{N}4-\text{C}5(\text{S}1)-$ ,  $\text{C}4-\text{N}3$  and  $\text{C}5-\text{S}1$  bond lengths values of  $1.283(2)\ \text{\AA}$  and  $1.697(1)\ \text{\AA}$  are consistent with double bond character, while  $\text{C}5-\text{N}4$  distance of  $1.350(2)\ \text{\AA}$  and  $\text{N}3-\text{N}4$  distance of  $1.367(2)\ \text{\AA}$  are indicative of a simple bond character. The same fact are observed in the second ligand molecule:  $\text{C}9-\text{N}8$  and  $\text{C}10-\text{S}2$  bond lengths values of  $1.286(2)\ \text{\AA}$  and  $1.711(1)\ \text{\AA}$  are consistent with double bond character while  $\text{C}10-\text{N}9$  distance of  $1.349(2)\ \text{\AA}$  and  $\text{N}8-\text{N}9$  distance of  $1.367(2)\ \text{\AA}$  are indicative of a simple bond character. All these observations show clearly that iminisation does not undergoes for the thiosemicarbazide moiety upon coordination and the sulfur atoms coordinate to the Ni(II) in their thione form as observed in a similar complex  $[\text{Ni}(\text{H}_2\text{L})_2]\cdot 2\text{Cl}$  where  $\text{H}_2\text{L}$  is 1-(1-hydroxypropan-2-ylidene)thiosemicarbazide [42]. Intermolecular hydrogen bonds involving the NH of the imidazole nitrogen, the NH of the hydrazine, and the NH of the amino groups of the ligand as donor and the chloride anion or the thione sulfur atom as acceptor:  $\text{N}7-\text{H}7\cdots\text{Cl}2^i$ ,  $i = -x+2, -y+1, -z$ ;  $\text{N}4-\text{H}4\cdots\text{Cl}1^{ii}$ ,  $\text{N}5-\text{H}5\text{A}\cdots\text{O}1^{iii}$ ;  $ii = -x+2, -y+2, -z+1$ ;  $\text{N}9-\text{H}9\cdots\text{Cl}2^{iii}$ ,  $\text{N}10-\text{H}10\text{A}\cdots\text{Cl}2^{iii}$ ;  $iii = -x+1, -y, -z$ ;  $\text{N}2-\text{H}2\cdots\text{S}2^{iv}$ ;  $iv = x+1, y, z$ ;  $\text{N}5-\text{H}5\text{B}\cdots\text{Cl}1^v$ ;  $v = x-1, y, z$ ;  $\text{N}10-\text{H}10\text{B}\cdots\text{Cl}1^{vi}$ ;  $vi = x-1, y-1, z$  (Table 3, Fig. 2) consolidate the structure in a three-dimensional network (Fig. 3).

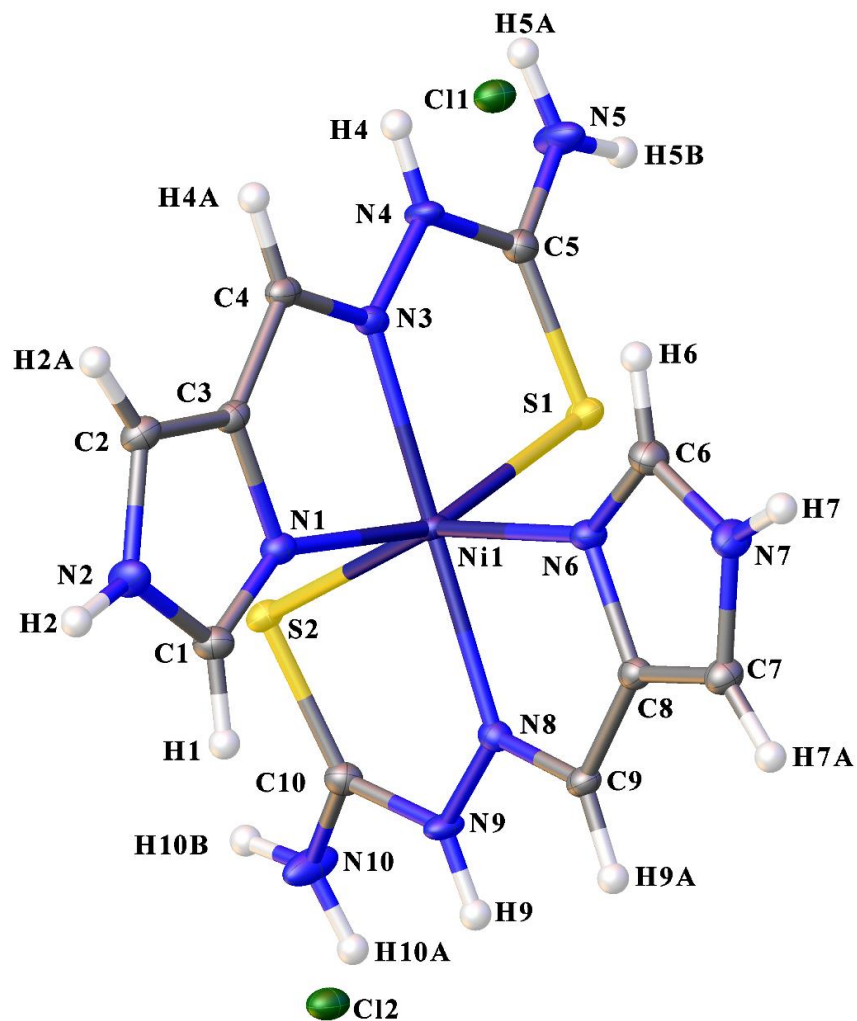


Figure 1: ORTEP plot (30% probability ellipsoids) showing the structure of (1).

Table-2. Selected bond lengths (Å) for complex 1.

Ni1—S2	2.4662 (4)	S2—C10	1.7112 (15)
Ni1—S1	2.4456 (4)	S1—C5	1.6975 (15)
Ni1—N8	2.0421 (12)	N8—N9	1.3673 (16)
Ni1—N3	2.0459 (12)	N8—C9	1.2860 (19)
Ni1—N6	2.0939 (12)	N3—N4	1.3674 (17)
Ni1—N1	2.0819 (12)	N3—C4	1.283 (2)
S1—Ni1—S2	92.746 (13)	N3—Ni1—N6	97.57 (5)
N8—Ni1—S2	80.44 (3)	N3—Ni1—N1	78.37 (5)
N8—Ni1—S1	102.89 (3)	N6—Ni1—S2	158.43 (3)
N8—Ni1—N3	174.64 (5)	N6—Ni1—S1	95.49 (3)
N8—Ni1—N6	78.30 (5)	N1—Ni1—S2	90.95 (3)
N8—Ni1—N1	97.98 (5)	N1—Ni1—S1	159.13 (3)
N3—Ni1—S2	103.42 (3)	N1—Ni1—N6	88.41 (5)
N3—Ni1—S1	80.80 (4)		

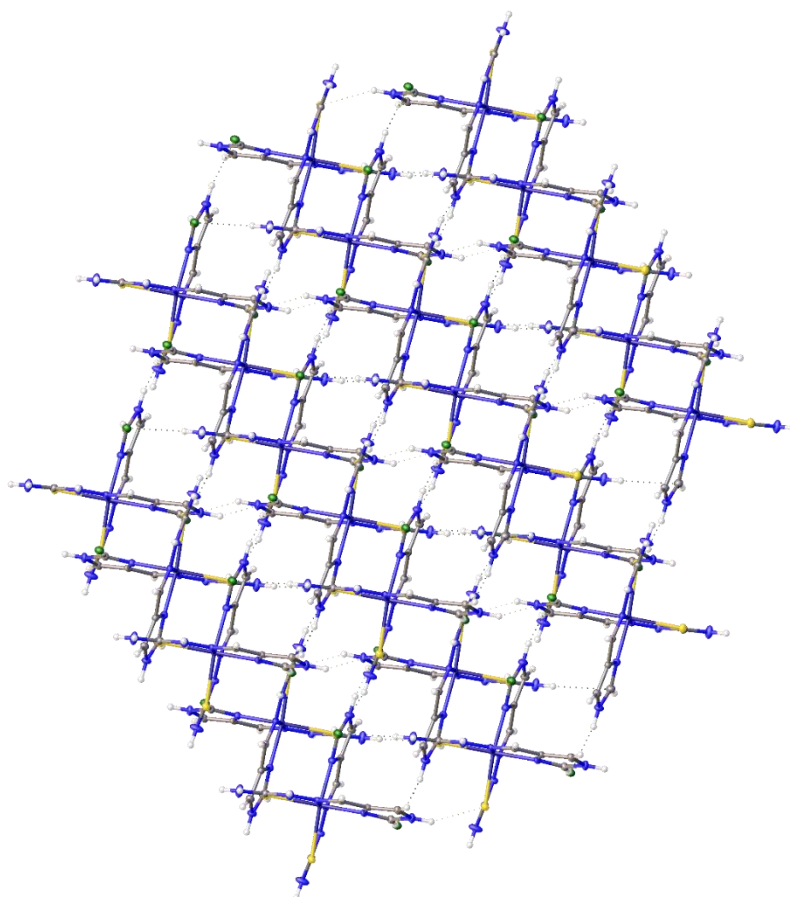


Figure 2: Plot showing the inter and intramolecular hydrogens bonds in the crystal.

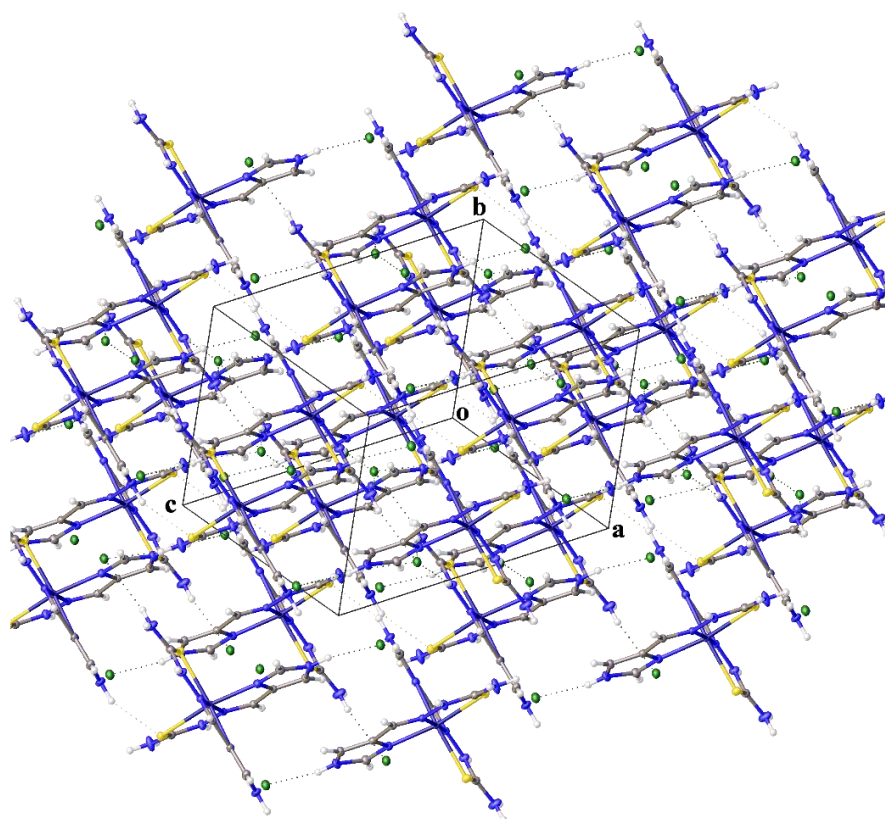


Figure 3. The packing of the complex (1) in the crystal structure.

**Table-3.** Intra and inter molecular hydrogen bonds.

<i>D—H...A</i>	<i>D—H</i>	<i>H...A</i>	<i>D...A</i>	<i>D—H...A</i>
N7—H7...Cl2 <sup>i</sup>	0.88	2.32	3.1857(13)	169.5
N4—H4...Cl1 <sup>ii</sup>	0.88	2.36	3.1719(12)	153.3
N9—H9...Cl2 <sup>iii</sup>	0.88	2.40	3.1966(12)	150.8
N2—H2...S2 <sup>iv</sup>	0.88	2.48	3.2896(13)	152.9
N5—H5A...Cl1 <sup>ii</sup>	0.88	2.40	3.2111(14)	153.9
N5—H5B...Cl1 <sup>v</sup>	0.88	2.58	3.3352(14)	144.7
N10—H10A...Cl2 <sup>iii</sup>	0.88	2.34	3.1647(14)	155.8
N10—H10B...Cl1 <sup>vi</sup>	0.88	2.31	3.1754(14)	167.1

Symmetry codes: (i)  $-x+2, -y+1, -z$ ; (ii)  $-x+2, -y+2, -z+1$ ; (iii)  $-x+1, -y, -z$ ; (iv)  $x+1, y, z$ ; (v)  $x-1, y, z$ ; (vi)  $x-1, y-1, z$ .

#### IV. Conclusion

The ligand 1-((1*H*-imidazol-4-yl)methylene)thiosemicarbazide (HL) and its nickel(II) complex [Ni(HL)<sub>2</sub>]-2Cl were synthesized and characterized with various physicochemical techniques such as elemental analyses, IR, NMR, and single crystal X-ray diffraction analysis. The metal atoms is bonded to each of the two ligand molecules by a nitrogen atom from the imidazole ring, the azomethine nitrogen atom and the thione sulfur atom from the S=C(NH<sub>2</sub>)-NH-N=C chromophore. Tus nickel(II) ion is hexacoordinated, yielding an octahedral geometry around the nickel(II) center. Two uncoordinated chloride anions are present as counter ions.

#### Supplementary Materials

CCDC-2253997 contains the supplementary crystallographic data for this paper. These data can be obtained free of charge via <https://www.ccdc.cam.ac.uk/structures/>, or by e-mailing [data\\_request@ccdc.cam.ac.uk](mailto:data_request@ccdc.cam.ac.uk), or by contacting The Cambridge Crystallographic Data Centre, 12 Union Road, Cambridge CB2 1EZ, UK; fax: +44(0)1223-336033.

#### References

- Alam, M., Abser, M. N., Kumer, A., Bhuiyan, M. M. H., Akter, P., Hossain, M. E., Chakma, U. (2023). Synthesis, Characterization, Antibacterial Activity Of Thiosemicarbazones Derivatives And Their Computational Approaches: Quantum Calculation, Molecular Docking, Molecular Dynamic, ADMET, QSAR. *Heliyon*, 9(6), E16222. <https://doi.org/10.1016/j.heliyon.2023.E16222>
- Santos, T. A. R. Dos, Silva, A. C. Da, Silva, E. B., Gomes, P. A. T. De M., Espíndola, J. W. P., Cardoso, M. V. De O., Moreira, D. R. M., Leite, A. C. L., Pereira, V. R. A. (2016). Antitumor And Immunomodulatory Activities Of Thiosemicarbazones And 1,3-Thiazoles In Jurkat And HT-29 Cells. *Biomedicine Pharmacotherapy*, 82, 555–560. <https://doi.org/10.1016/j.biopha.2016.05.038>
- Chellan, P., Land, K. M., Shokar, A., Au, A., An, S. H., Clavel, C. M., Dyson, P. J., De Kock, C., Smith, P. J., Chibale, K., Smith, G. S. (2012). Exploring The Versatility Of Cycloplatinated Thiosemicarbazones As Antitumor And Antiparasitic Agents. *Organometallics*, 31(16), 5791–5799. <https://doi.org/10.1021/om300334z>
- Kaushik, S., Paliwal, S. K., Iyer, M. R., Patil, V. M. (2023). Promising Schiff Bases In Antiviral Drug Design And Discovery. *Medicinal Chemistry Research*, 32(6), 1063–1076. <https://doi.org/10.1007/s00044-023-03068-0>
- Combination Of N-Methylisatin-B-Thiosemicarbazone Derivative (SCH16) With Ribavirin And Mycophenolic Acid Potentiates The Antiviral Activity Of SCH16 Against Japanese Encephalitis Virus In Vitro. (2012). Sebastian, L., Desai, A., Yogeewari, P., Sriram, D., Madhusudana, S.N., Ravi, V. *Letters In Applied Microbiology*, 55(3), 234–239. <https://doi.org/10.1111/j.1472-765x.2012.03282.x>
- D'Agostino, I., Mathew, G. E., Angelini, P., Venanzoni, R., Flores, G. A., Angeli, A., Carradori, S., Marinacci, B., Menghini, L., Abdelgawad, M. A., Ghoneim, M. M., Mathew, B., Claudiu, T. S., Supuran, C. T. (2022). Biological Investigation Of N-Methyl Thiosemicarbazones As Antimicrobial Agents And Bacterial Carbonic Anhydrases Inhibitors. *Journal Of Enzyme Inhibition And Medicinal Chemistry*, 37(1), 986–993. <https://doi.org/10.1080/14756366.2022.2055009>
- Hossan, A. (2023). Microwave-Assisted Solvent-Free Synthesis Of Some Novel Thiazole-Substituted Thiosemicarbazone Analogues: Antimicrobial And Anticancer Studies. *Luminescence*, 2023, 1-13. <https://doi.org/10.1002/bio.4587>
- Mallikarjuna, B. P., Sastry, B. S., Kumar, G. V. S., Rajendraprasad, Y., Chandrashekar, S. M., Sathisha, K. (2009). Synthesis Of New 4-Isopropylthiazole Hydrazide Analogs And Some Derived Clubbed Triazole, Oxadiazole Ring Systems – A Novel Class Of Potential Antibacterial, Antifungal And Antitubercular Agents. *European Journal Of Medicinal Chemistry*, 44(11), 4739–4746. <https://doi.org/10.1016/j.ejmech.2009.06.008>
- Mangawa, S. K., Singh, S. (2023). Ferrocene Derivatives As New Generation Of Antimalarial Agents: Opportunity Or Illusion? *Current Topics In Medicinal Chemistry*, 23(16), 1503–1521. <https://doi.org/10.2174/1568026623666230228153114>

- [10]. Datta, S., Seth, D. K., Gangopadhyay, S., Karmakar, P., Bhattacharya, S. (2012). Nickel Complexes Of Some Thiosemicarbazones: Synthesis, Structure, Catalytic Properties And Cytotoxicity Studies. *Inorganica Chimica Acta*, 392, 118–130. <https://doi.org/10.1016/j.ica.2012.05.034>
- Chikate, R. C., Padhye, S. B. (2005). Transition Metal Quinone–Thiosemicarbazone Complexes 2: Magnetism, ESR And Redox Behavior Of Iron (II), Iron (III), Cobalt (II) And Copper (II) Complexes Of 2-Thiosemicarbazido-1,4-Naphthoquinone. *Polyhedron*, 24(13), 1689–1700. <https://doi.org/10.1016/j.poly.2005.04.037>
- [11]. Gil-García, R., Gómez-Saiz, P., Díez-Gómez, V., Madariaga, G., Insausti, M., Lezama, L., Cuevas, J. V., García-Tojal, J. (2014). Thiosemicarbazonecopper(II) Compounds With Halide/Hexafluorosilicate Anions: Structure, Water Clusters, Non-Covalent Interactions, And Magnetism. *Polyhedron*, 81, 675–686. <https://doi.org/10.1016/j.poly.2014.07.032>
- [12]. Alshater, H., Al-Sulami, F. I., Aly, S. A., Abdalla, E. M., Sakr, M. A., Hassan, S. S. (2023). Antitumor And Antibacterial Activity Of Ni(II), Cu(II), Ag(I), And Hg(II) Complexes With Ligand Derived From Thiosemicarbazones: Characterization And Theoretical Studies. *Molecules*, 28(6). <https://doi.org/10.3390/molecules28062590>
- [13]. Ozturk, I. I., Turk, K., Grzeskiewicz, A. M., Kubicki, M., Banti, C. N., Hadjikakou, S. K. (2023). Heteroleptic Six-Coordinate Bismuth(III) Complexes With 2-Acetylthiophene Thiosemicarbazones: Synthesis, Characterization, And Biological Properties. *New Journal Of Chemistry*, 47(27), 12779–12789. <https://doi.org/10.1039/D3NJ01411H>
- [14]. Gholizadeh, S., Eslami, F., Arami, S., Dehghan, G., Hosseini-Yazdi, S. A., Tackallou, S. H., Mahdavi, M. (2023). Nickel (II) Phenylthiosemicarbazone Complex Induces Cytotoxicity, Oxidative Stress And Apoptosis In Human Leukemia Stem-Like KG1a Cells. *Iranian Journal Of Science*, 47(4), 1125–1135. <https://doi.org/10.1007/S40995-023-01509-4>
- [15]. Savir, S., Wei, Z. J., Liew, J. W. K., Vythilingam, I., Lim, Y. A. L., Saad, H. M., Sim, K. S., Tan, K. W. (2020). Synthesis, Cytotoxicity, And Antimalarial Activities Of Thiosemicarbazones And Their Nickel (II) Complexes. *Journal Of Molecular Structure*, 1211, 128090. <https://doi.org/10.1016/j.molstruc.2020.128090>
- [16]. Nguyen, M.-H., Khuat, T.-T.-H., Nguyen, H.-H., Phung, Q.-M., Dinh, T.-H. (2019). Emissive Pd(II) Thiosemicarbazones Bearing Anthracene: New Complexes With Unusual Coordination Mode. *Inorganic Chemistry Communications*, 102, 120–125. <https://doi.org/10.1016/j.inoche.2019.02.028>
- [17]. Nongpiur, C. G. L., Diengdoh, D. F., Banothu, V., Gannon, P. M., Kaminsky, W., Kollipara, M. R. (2023). Variable Coordination Behavior Of Rhodium Metal Complexes Towards Thiourea Derivative Ligands In Comparison To Its Ruthenium And Iridium Analogs: Synthesis And Biological Studies. *Journal Of Organometallic Chemistry*, 999, 122823. <https://doi.org/10.1016/j.jorganchem.2023.122823>
- [18]. Nongpiur, C. G. L., Ghate, M. M., Tripathi, D. K., Poluri, K. M., Kaminsky, W., Kollipara, M. R. (2022). Study Of Versatile Coordination Modes, Antibacterial And Radical Scavenging Activities Of Arene Ruthenium, Rhodium And Iridium Complexes Containing Fluorenone Based Thiosemicarbazones. *Journal Of Organometallic Chemistry*, 957, 122148. <https://doi.org/10.1016/j.jorganchem.2021.122148>
- [19]. Salsi, F., Roca Jungfer, M., Hagenbach, A., Abram, U. (2020). Trigonal-Bipyramidal Vs. Octahedral Coordination In Indium(III) Complexes With Potentially S,N,S-Tridentate Thiosemicarbazones. *European Journal Of Inorganic Chemistry*, 2020(13), 1222–1229. <https://doi.org/10.1002/ejic.201901356>
- [20]. Blagov, M. A., Spitsyna, N. G., Ovanesyana, N. S., Lobach, A. S., Zorina, L. V., Simonov, S. V., Zakharov, K. V., Vasiliev, A. N. (2023). First Crystal Structure Of An Fe(III) Anionic Complex Based On A Pyruvic Acid Thiosemicarbazone Ligand With Li<sup>+</sup>: Synthesis, Features Of Magnetic Behavior And Theoretical Analysis. *Dalton Trans.*, 52(6), 1806–1819. <https://doi.org/10.1039/D2DT03630D>
- [21]. Yousef, T. A., El-Reash, G. M. A., Morshedy, R. M. E. (2013). Structural, Spectral Analysis And DNA Studies Of Heterocyclic Thiosemicarbazone Ligand And Its Cr(III), Fe(III), Co(II) Hg(II), And U(VI) Complexes. *Journal Of Molecular Structure*, 1045, 145–159. <https://doi.org/10.1016/j.molstruc.2013.03.060>
- [22]. Jeong, H., Kang, Y., Kim, J., Kim, B.-K., Hong, S. (2019). Factors That Determine Thione(Thiol)–Disulfide Interconversion In A Bis(Thiosemicarbazone) Copper(II) Complex. *RSC Advances*, 9(16), 9049–9052. <https://doi.org/10.1039/C9RA01115C>
- [23]. Santoro, A., Vileno, B., Palacios, Ò., Peris-Díaz, M. D., Riegel, G., Gaiddon, C., Krężel, A., Faller, P. (2019). Reactivity Of Cu(II)–, Zn(II)– And Fe(II)–Thiosemicarbazone Complexes With Glutathione And Metallothionein: From Stability To Dissociation To Transmetallation†. *Metallomics*, 11(5), 994–1004. <https://doi.org/10.1039/C9mt00061e>
- [24]. Raman, N., Selvan, A., Manisankar, P. (2010). Spectral, Magnetic, Biocidal Screening, DNA Binding And Photocleavage Studies Of Mononuclear Cu(II) And Zn(II) Metal Complexes Of Tricoordinate Heterocyclic Schiff Base Ligands Of Pyrazolone And Semicarbazide/Thiosemicarbazide Based Derivatives. *Spectrochimica Acta Part A: Molecular And Biomolecular Spectroscopy*, 76(2), 161–173. <https://doi.org/10.1016/j.saa.2010.03.007>
- [25]. Ain, Q. U., Sharma, R. (2023). Structure And Bonding Trends Of Bisthiosemicarbazones: An Overview. *Applied Organometallic Chemistry*, 37(6), E7100. <https://doi.org/10.1002/Aoc.7100>
- [26]. Angupillai, S., Hwang, J.-Y., Lee, J.-Y., Rao, B. A., Son, Y.-A. (2015). Efficient Rhodamine-Thiosemicarbazide-Based Colorimetric/Fluorescent ‘Turn-On’ Chemodosimeters For The Detection Of Hg<sup>2+</sup> In Aqueous Samples. *Sensors And Actuators B: Chemical*, 214, 101–110. <https://doi.org/10.1016/j.snb.2015.02.126>
- [27]. Shaikh, A., Mukherjee, P., Ta, S., Bhattacharyya, A., Ghosh, A., Das, D. (2020). Oxidative Cyclization Of Thiosemicarbazide: A Chemodosimetric Approach For The Highly Selective Fluorescence Detection Of Cerium(IV). *New Journal Of Chemistry*, 44(22), 9452–9455. <https://doi.org/10.1039/D0NJ01100B>
- [28]. Pouramiri, B., Kermani, E. T. (2017). Lanthanum(III) Chloride/Chloroacetic Acid As An Efficient And Reusable Catalytic System For The Synthesis Of New 1-((2-Hydroxynaphthalen-1-Yl)(Phenyl)methyl)Semicarbazides/Thiosemicarbazides. *Arabian Journal Of Chemistry*, 10, S730–S734. <https://doi.org/10.1016/j.arabjc.2012.11.016>

- Maurya, M. R., Sarkar, B., Kumar, A., Ribeiro, N., Miliute, A., Pessoa, J. C. (2019). New Thiosemicarbazide And Dithiocarbamate Based Oxidovanadium(IV) And Dioxidovanadium(V) Complexes. Reactivity And Catalytic Potential. *New Journal Of Chemistry*, 43(45), 17620–17635.  
<https://doi.org/10.1039/C9NJ01486A>
- [29]. Sheldrick, G. M. (2015). Integrated Space-Group And Crystal-Structure Determination. *Acta Crystallographica Section A*, 71(1), 3–8.  
<https://doi.org/10.1107/S2053229614024218>
- [30]. Sheldrick, G. M. (2015). Crystal Structure Refinement With SHELXL. *Acta Crystallographica Section C*, 71(1), 3–8.  
<https://doi.org/10.1107/S2053273314026370>
- [31]. Farrugia, L. J. (2012). Wingx And ORTEP For Windows: An Update. *Journal Of Applied Crystallography*, 45(4), 849–854.  
<https://doi.org/10.1107/S0021889812029111>
- [32]. Singh, A. K., Pandey, O. P., Sengupta, S. K. (2013). Synthesis, Spectral And Antimicrobial Activity Of Zn(II) Complexes With Schiff Bases Derived From 2-Hydrazino-5-[Substituted Phenyl]-1,3,4-Thiadiazole And Benzaldehyde/2-Hydroxyacetophenone/Indoline-2,3-Dione. *Spectrochimica Acta Part A: Molecular And Biomolecular Spectroscopy*, 113, 393–399.  
<https://doi.org/10.1016/J.Saa.2013.04.045>
- [33]. Joshi, R., Kumari, A., Singh, K., Mishra, H., Pokharia, S. (2019). Synthesis, Structural Characterization, Electronic Structure Calculation, Molecular Docking Study And Biological Activity Of Triorganotin(IV) Complexes Of Schiff Base (E)-4-Amino-3-(2-(2-Hydroxybenzylidene)hydrazinyl)-1H-1,2,4-Triazole-5(4H)-Thione. *Journal Of Molecular Structure*, 1197, 519–534.  
<https://doi.org/10.1016/J.Molstruc.2019.07.066>
- [34]. Haba, P., Sy, A., Tamboura, F. B., Sarr, M., Thiam, I. E., Barry, A. H., Sall, M. L., Gaye, M., Retailleau, P. (2019). Synthesis, Spectroscopic Studies, And X-Ray Structure Determination Of Two Mononuclear Copper Complexes Derived From The Schiff Base Ligand N,N-Dimethyl-N'-(5-Methyl-1H-Imidazol-4-Yl)methylene)ethane-1,2-Diamine. *European Journal Of Chemistry*, 10(3), 201–208.  
<https://doi.org/10.5155/Eurjchem.10.3.201-208.1881>
- [35]. Geary, W. J. (1971). The Use Of Conductivity Measurements In Organic Solvents For The Characterisation Of Coordination Compounds. *Coordination Chemistry Reviews*, 7(1), 81–122.  
[https://doi.org/10.1016/S0010-8545\(00\)80009-0](https://doi.org/10.1016/S0010-8545(00)80009-0)
- [36]. Hadadzadeh, H., Mansouri, G., Rezvani, A., Khavasi, H. R., Skelton, B. W., Makha, M., Charati, F. R. (2011). Mononuclear Nickel(II) Complexes Coordinated By Polypyridyl Ligands. *Polyhedron*, 30(15), 2535–2543.  
<https://doi.org/10.1016/J.Poly.2011.06.037>
- [37]. Netalkar, P. P., Netalkar, S. P., Revankar, V. K. (2015). Transition Metal Complexes Of Thiosemicarbazone: Synthesis, Structures And Invitro Antimicrobial Studies. *Polyhedron*, 100, 215–222.  
<https://doi.org/10.1016/J.Poly.2015.07.075>
- [38]. Netalkar, P. P., Netalkar, S. P., Revankar, V. K. (2015). Transition Metal Complexes Of Thiosemicarbazone: Synthesis, Structures And Invitro Antimicrobial Studies. *Polyhedron*, 100, 215–222.  
<https://doi.org/10.1016/J.Poly.2015.07.075>